**Plant Communications, Volume *3***

## Supplemental information

# Genome-edited ATP BINDING CASSETTE B1 transporter SD8 knock-outs show optimized rice architecture without yield penalty

**Ruihong Qu, Pingxian Zhang, Qing Liu, Yifan Wang, Weijun Guo, Zhuoying Du, Xiulan Li, Liwen Yang, Shuangyong Yan, and Xiaofeng Gu**

SUPPLEMENTAL INFORMATION

# Genome-edited ATP BINDING CASSETTE B1 transporter SD8 knockouts have optimized rice architecture without yield penalty

Ruihong Qu[1,5], Pingxian Zhang[2,5], Qing Liu[4,5], Yifan Wang[1], Weijun Guo[1], Zhuoying Du[1], Xiulan Li[1], Liwen Yang[1,*], Shuangyong Yan[3,*], Xiaofeng Gu[1,*]

[1]Biotechnology Research Institute, Chinese Academy of Agricultural Science, Beijing 100081, China

[2]College of Life Science and Technology, Huazhong Agricultural University, Wuhan 430070, Hubei, China

[3]Tianjin Key Laboratory of Crop Genetics and Breeding, Tianjin Crop Research Institute, Tianjin Academy of Agricultural Sciences, Tianjin 300384, China

[4]College of life sciences, Hebei agricultural university, Baoding 071001, Hebei, China

[5]These authors contributed equally.

***Correspondence:** Liwen Yang (yangliwen@caas.cn), Shuangyong Yan (bioysy@139.com), Xiaofeng Gu (guxiaofeng@caas.cn)

**This PDF file includes:**

SI Materials and Methods

Figures S1 to S11 and Tables S1

SI References

**List of Supplemental Information:**

## SI Materials and Methods

### Plant materials and growth conditions

In this study, seven cultivars of rice (*Oryza sativa* L.) were used for creating CRISPR/Cas9 gene-editing lines, namely, three *japonica* cultivars Nipponbare (NIP), Jinggeng818 (JG), and Longgeng31 (LG), and four *indica* cultivars 9311, YexiangB (YX), Nongxiang32 (NX), and Yuzhenxiang (YZX). For phenotypic analysis, the plants were spaced 30 cm apart and grown at the Chinese Academy of Agricultural Sciences in Beijing (39°54'N, 116°23'E), China, from May to October of each year. For hormone analysis, rice plants were planted in water-soaked sand for germination, and after 3 days seeds were transferred into normal culture solution. Rice plants were grown in growth chambers with 60–70% humidity and a light/dark cycle of 12/12 h at 30/24°C.

### Transgene constructs and targeted gene editing

To generate knockout plants using CRISPR/Cas9 technology, single-guide RNA targeting 5′- GCTGGACGGCCACGACCTGA -3′ was cloned downstream of the *OsU6* promoter in the CRISPR/Cas9 binary vector BGK032 (Biogle Technology). These constructs were introduced into diverse rice backgrounds (two *japonica* varieties (Jingeng818 (JG) and Longgeng31 (LG)) and four *indica* varieties (Nongxiang32 (NX), 93-11, YexiangB (YX), and Yuzhenxiang (YZX)) by Agrobacterium-mediated transformation using standard protocols. For complementation of the *SD8-1* mutant, a DNA fragment containing the 2000 bp promoter and the full-length protein-coding sequence of *SD8*/*OsABCB1* (CDS: 4,035 bp) was amplified and inserted into a binary vector p23A between KpnI sites. For *SD8* overexpression, the full-length

*SD8*/*OsABCB1* protein-coding sequence was amplified from NIP and cloned into the vector pBS-2, then introduced into the plant binary vector pCAMBIA1304 to generate the fusion *pCaMV35S::SD8*. The transgenic rice plants were confirmed by quantitative real-time PCR (qPCR) or PCR detection and direct sequencing.

**Subcellular localization**

A vector containing *p35S::SD8-GFP* was transiently expressed in rice protoplasts as described previously (Geng et al., 2020; Zhang et al., 2021). GFP fluorescence signals were observed and recorded using a Zeiss LSM 700 confocal laser-scanning microscope.

***Pro: SD8-GUS* analysis**

The *proSD8::GUS* transgenic plants were grown in standard rice culture solution. GUS staining of tissues was carried out as described previously (Zhang et al., 2021).

**qRT-PCR assays**

Total RNA was prepared using RNeasy Plant Mini kit (Qiagen) and then contaminating genomic DNA was removed by digestion with recombinant DNase I (RNase-free, TAKARA) following the manufacturer's instructions. qRT-PCR was performed using SYBR Green Supermix (TOYOBO) on an Applied Biosystems 7500 Fast real-time PCR system. Relative expression of the selected genes was analyzed using the $2^{-\Delta\Delta CT}$ method (Zhang et al., 2021).

**Quantification of IAA content and flux in rice plants**

Endogenous free IAA in rice plant 3 weeks seedling were quantified by gas chromatography-mass spectrometry (GC-MS) as described in Henrichs et al. (2012).

The measurements were carried out using a GC-MS system at the Central Laboratory of Biotechnology Research Institute, Chinese Academy of Agricultural Sciences.

IAA fluxes were monitored non-invasively in the roots of plants grown for 7 days in hydroponic solutions using SIET (model BIO-003A; Younger USA Science and Technology, Falmouth, MA, USA, and Xu-Yue Science and Technology, Beijing, China; http://www.xuyue.net) containing an IAA-sensitive amperometric sensor based on a carbon nanotube-coated external oxidizing platinum microelectrode as described previously (Henrichs et al., 2012; Yang et al.,2020). The net influx current was defined as the difference between currents recorded in the absence and presence of exogenous 10 mM IAA. Fluxes were measured in the roots of at least 6-10 individual plants in two independent experiments.

**SD8/OsABCB1 functionality assays for auxin acquisition in the IAA-sensitive yeast strain *yap1-1***

The whole open reading frames of *SD8* was amplified by PCR from cDNA of rice using forward primers SD8F (5'-CGGAATTCATGGAGGAGGAGATAAAGGG-3'), with an EcoRI site incorporated at the 5' end, and reverse primers SD8R (5'-CCG CTCGAGCTAGGTGCCGTGTGTTGTTGTTG-3'), with an XhoI site incorporated at the 3' end. After EcoRI and XhoI double enzyme digestion, the fragment was inserted between the EcoRI and XhoI sites of yeast expression vectors pYES2 and pDR196 (Yang et al., 2014). Subsequently, plasmids of pYES2, pDR196, *pYES2-SD8*, and *pDR196-SD8* were transformed into the IAA-sensitive mutant strain (S. cerevisiae) yap1-1 (Prusty et al., 2004) as described previously (Yang et al., 2014). Positive transformants were selected on glucose containing solid SD-U medium without uracil, and single colonies were grown in liquid SD-U medium supplemented with 2%

galactose or glucose. For functionality assays, transformants grown in liquid SD-U medium to an OD600 of approximately 0.6 were washed and diluted to OD600 in deionized water. Cells were diluted 10-fold three times, and 3 ml of each dilution was spotted onto an SD-U medium plate supplemented with the indicated concentrations of IAA. The plates were incubated at 30℃ for 3-5 days. The assays were performed with three independent transformants.

**Yield-related trait measurements**

All yield traits were measured when the plants had attained maturity. Panicle length, grain length, yield per plant, seed setting rate, and 1,000-grain weight were recorded. Yield per plant was scored as the total weight of grains from the entire plant. The number of tillers per plant was scored as the number of reproductive tillers for each plant. And 1,000-grain weight were measured using an automatic seed counting and analyzing instrument (Model SC-G; Wanshen). Plant height and panicle length were measured and analyzed.

**GWAS analysis**

The SNPs data on rice height (at the mature stage) were originated from previously reported 3k RG database (Wang et al., 2018). Briefly, we selected 3k RG 404k Core SNPs (MAF > 0.05 and missing rate <50%) to perform GWAS of plant height. The GWAS was conducted with a mixed linear model that was implemented in TASSEL v5.0 (Bradbury et al., 2007). We then selected $p=2.78\times10^{-5}$ (Benjamini–Hochberg FDR < 0.05) as the genome-wide significant cutoff followed by a previously conducted GWAS analysis (Duan et al., 2017).

**Population genetic analysis of *SD8***

The haplotypes of *SD8* in the 3k RG were classified according to all SNPs with minor allele frequency>0.01 within the CDS region using the RFGB v2.0 database. The haplotypes in at least 100 rice accessions were used for comparative analysis of plant height traits, which were downloaded from the Rice SNP-Seek Database (Alexandrov N et al., 2015). One-way ANOVA followed by Duncan's new multiple-range test was performed with the agricolae package in *R*. Haplotype networks were constructed using the pegas package in *R*. Nucleotide diversity ($\pi$) and Tajima's D for each 50-kb window across the genome, with an overlapping 5-kb step size, were calculated for the 2-Mb region flanking *SD8* with the Variscan software (v2.0.3) (Vilella A et al.,2005).

**Yield evaluation under different planting densities**

Paddy trials were performed at the Chinese Academy of Agricultural Sciences in Beijing (39°54'N, 116°23'E), China, from May to October of each year. For NIP and *sd8-1* lines, each rice plant was grown in a paddy field at a distance of 20x10 cm (280,000 plants/ha), and 20x5 cm (560,000 plants/ha). Each treatment was performed in three individual plots with randomized blocks. A hundred rice plants were harvested and used for analysis from each plot excluding marginal plants. After harvest, the samples were dried for 14 days at 37℃ prior to measurements.

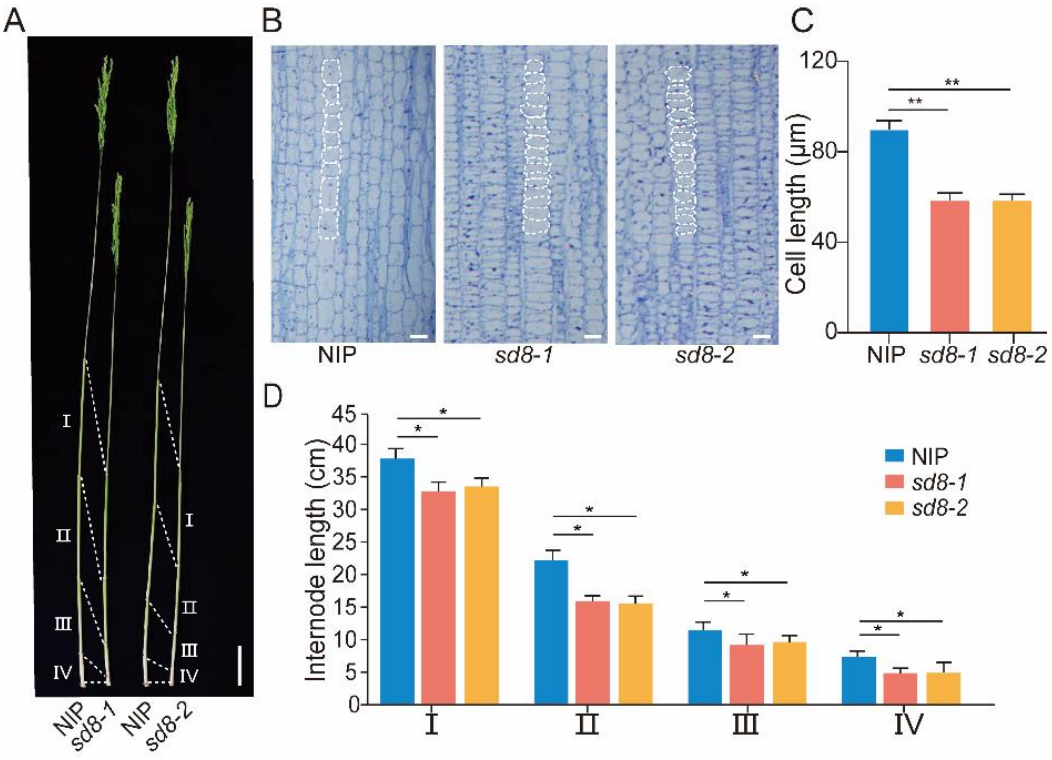


**Supplementary Figure 1. *SD8* knockout (KO) lines reduced the length of the main culms.**

**(A)** Main culms of wild-type (NIP) and *SD8* knockout lines (*sd8-1* and *sd8-2*). Arrows indicate nodes (scale bar:10 cm).

**(B)** Longitudinal sections of the elongated regions of the uppermost internodes of NIP, *sd8-1,* and *sd8-2* (Scale bars:50 μm for the longitudinal sections).

**(C)** Statistical data of the cell length in the longitudinal sections in B.

**(D)** Internode lengths of *SD8* KO lines (*sd8-1* and *sd8-2*) and NIP rice plants. Data indicate mean ± SD (n = 18). (**$p < 0.01$; *$p < 0.05$, Student's *t*-test).

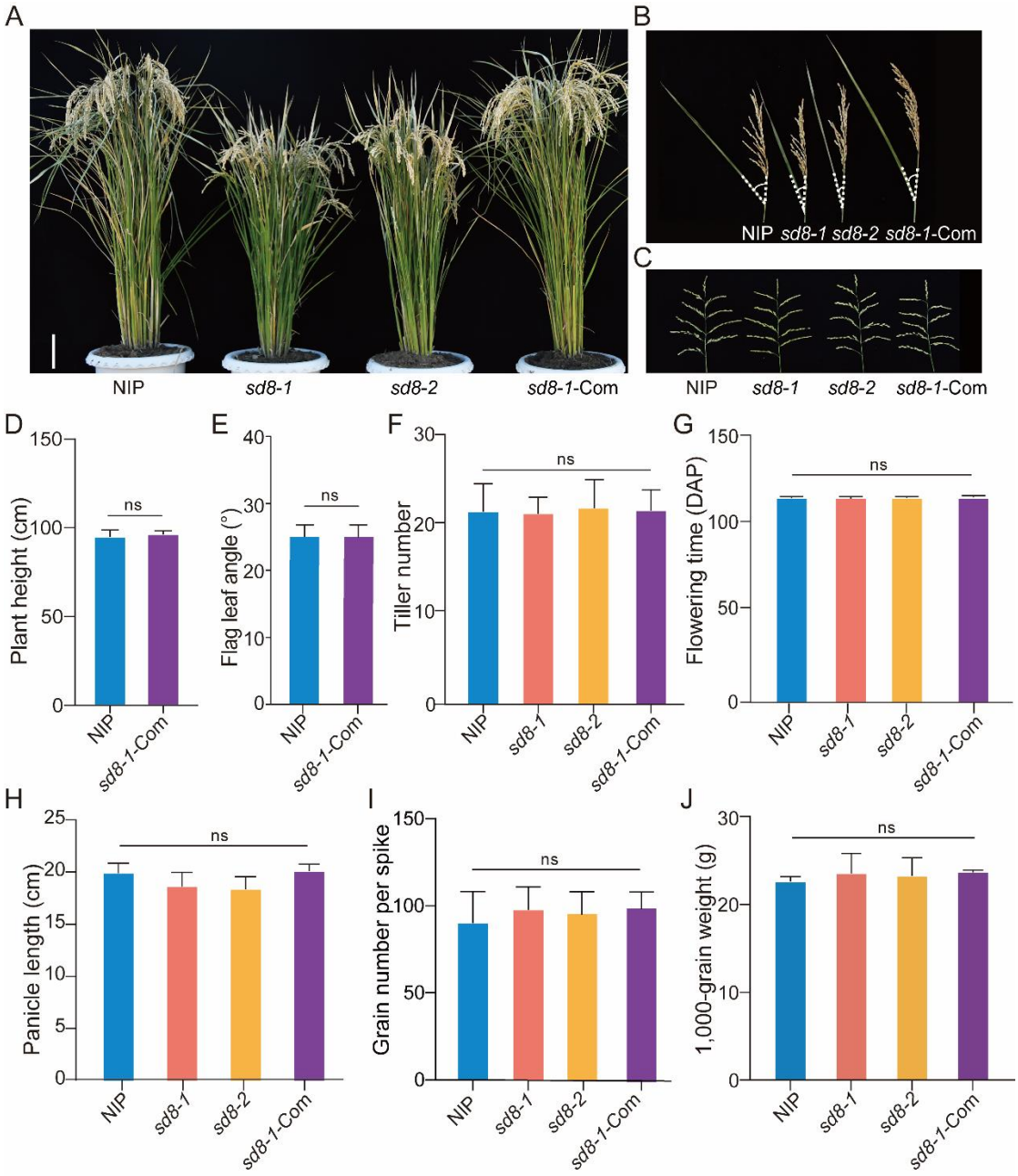


**Supplementary Figure 2. Phenotypes of *SD8* KO and complemented lines.**

**(A)** Plant architecture of mature stage NIP, *sd8-1*, *sd8-2,* and *sd8-1*-Com. (scale bar: 10 cm).

**(B)** The flag leaf angle in NIP, *sd8-1*, *sd8-2,* and *sd8-1*-Com plants.

**(C)** The panicle morphology in NIP, *sd8-1*, *sd8-2,* and *sd8-1*-Com plants.

**(D)** Comparison of plant height between NIP and *sd8-1*-Com.

**(E)** Comparison of flag angle between NIP and *sd8-1*-Com.

**(F-J)** Comparison of tiller number, flowering time, panicle length, grain number per spike, and 1,000-grain weight in NIP, *sd8-1*, *sd8-2,* and *sd8-1*-Com. Data represent

mean ± SD (n=24). (**$p < 0.01$; *$p < 0.05$, Student's *t*-test).

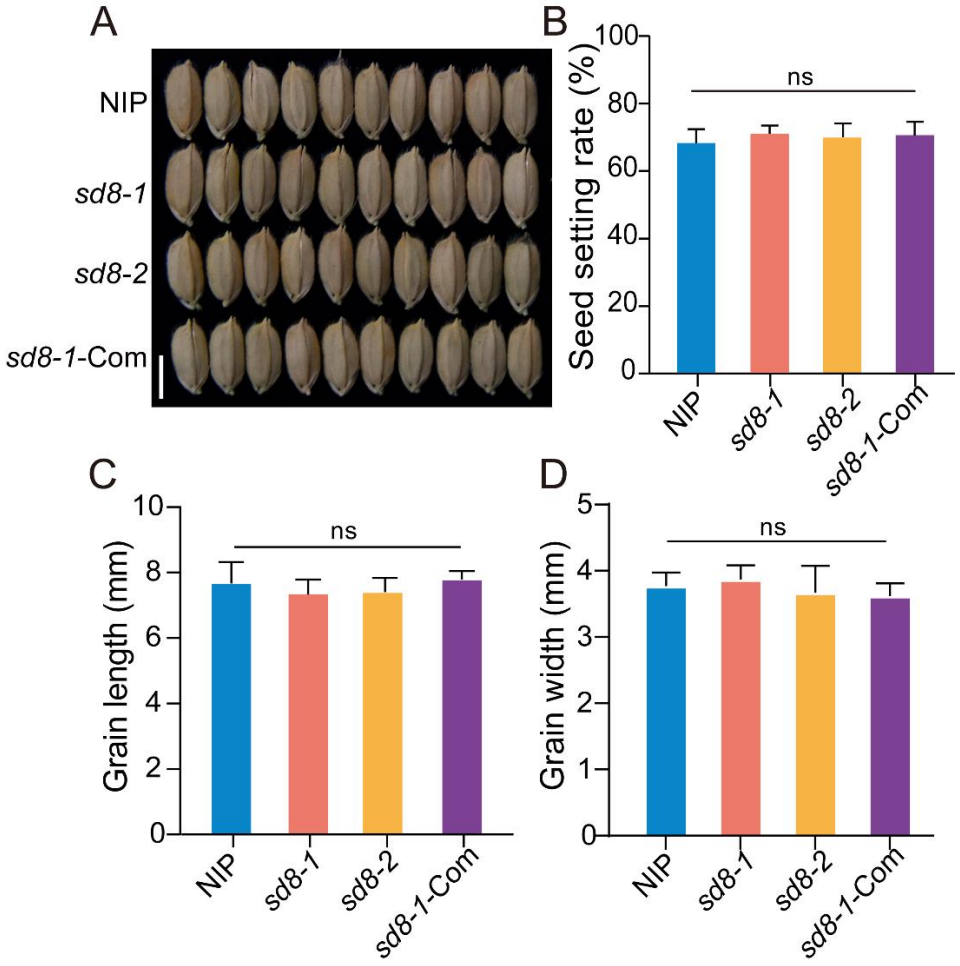


**Supplementary Figure 3. *SD8* KO lines did not cause significant differences in grain morphology compared to NIP.**

**(A)** Grain morphology of NIP, *sd8-1*, *sd8-2*, and *sd8-1*-Com. (Scale bar:0.5 cm).

**(B)** Comparison of seed setting rate in NIP, *sd8-1*, *sd8-2*, and *sd8-1*-Com. Data represent mean ± SD (n = 24).

**(C-D)** Statistical data of the grain length (C) and width (D). (**$p < 0.01$; *$p < 0.05$, Student's *t*-test).

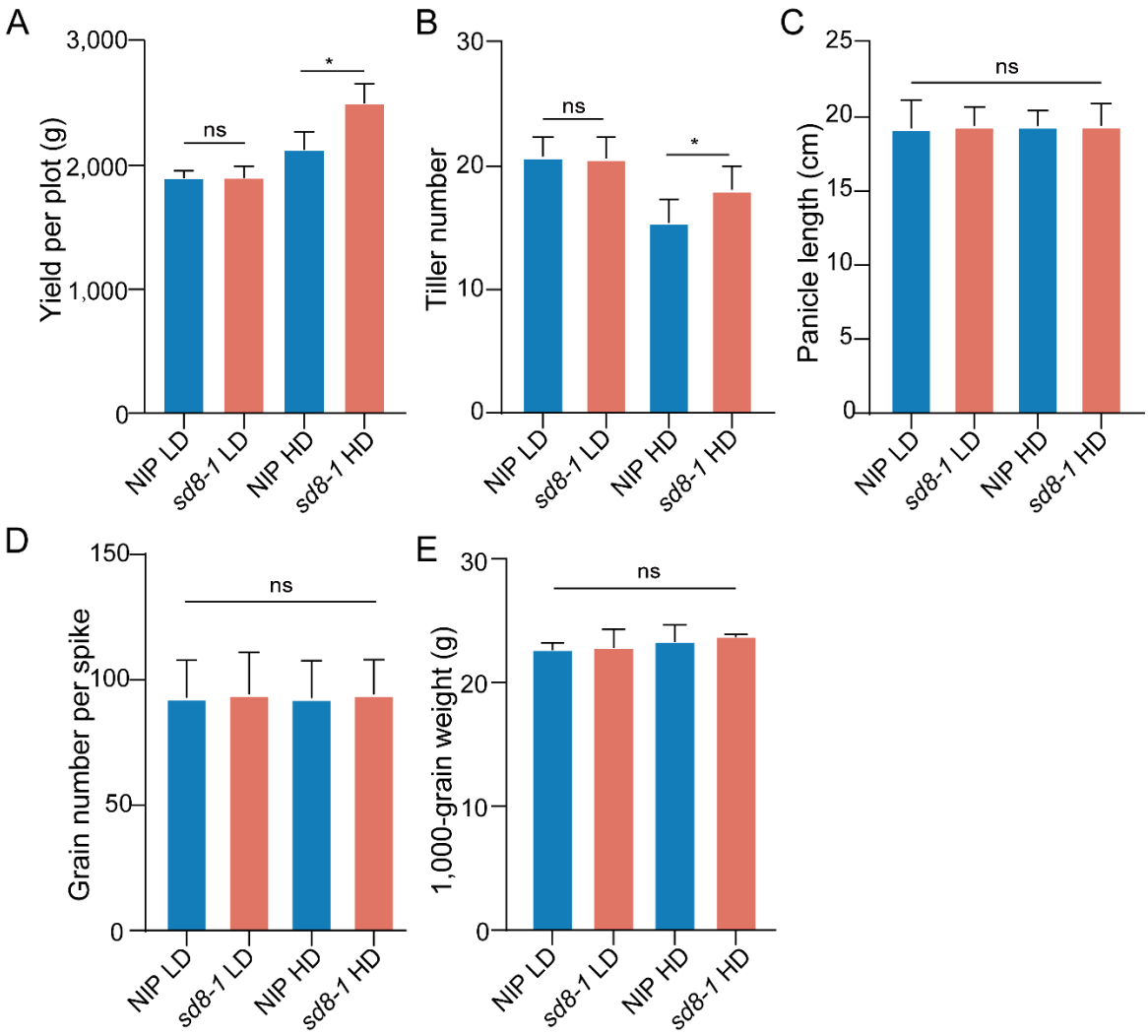


**Supplementary Figure 4. Statistical data of grain yield per plot and yield-related traits in NIP and *sd8-1* under different planting density conditions.**

**(A)** Grain yield per plot at high and low densities.

**(B-E)** Statistical data of yield-related traits in NIP and *sd8-1* under different planting density conditions. Different characters indicate significant differences. (**$p < 0.01$; *$p < 0.05$, Student's *t*-test).

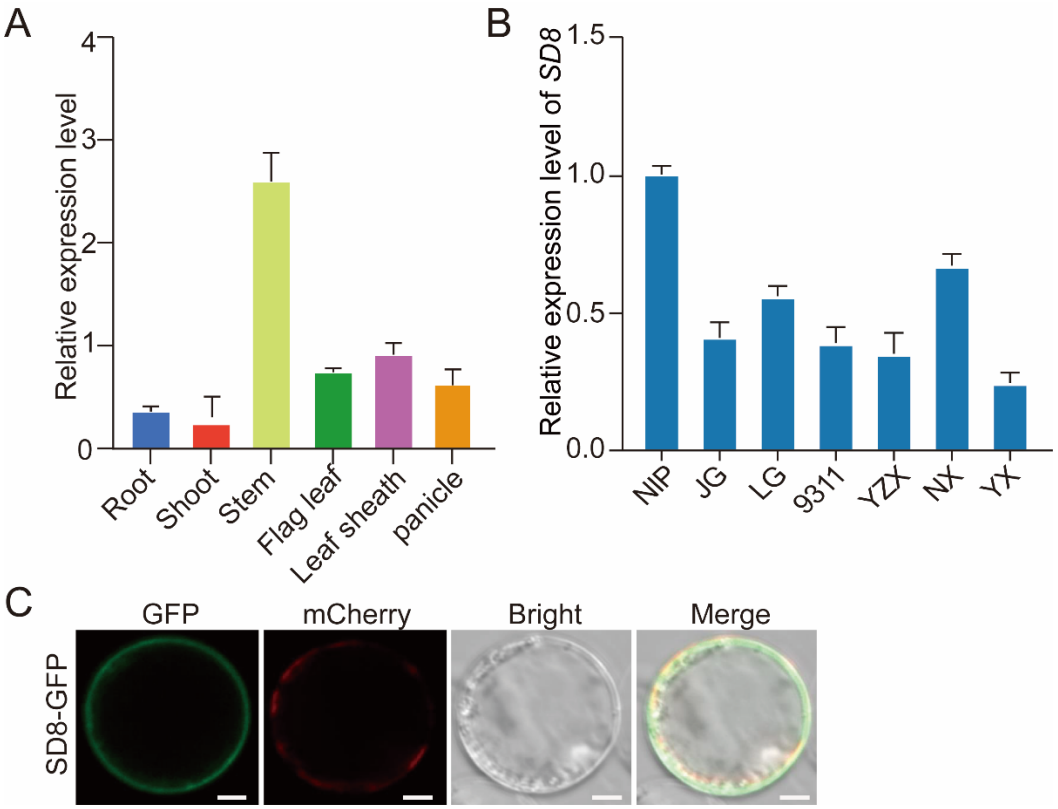


**Supplementary Figure 5. Expression pattern of *SD8* and subcellular location of SD8.**

**(A)** Relative expression level of *SD8* in each tissue of NIP at different growth stages. NIP was cultivated in normal culture solution for 3 weeks and transferred to the field. **(B)** Quantitative real-time PCR (qPCR) analysis of expression level of *SD8* between *indica* (9311, YZX, NX, YX) and *japonica* (NIP, JG, LG) rice varieties. All qRT-PCR experiments were analyzed using three independent biological repeats. **(C)** Subcellular localization of SD8/OsABCB1 in rice protoplasts. (Scale bars:10 μm).

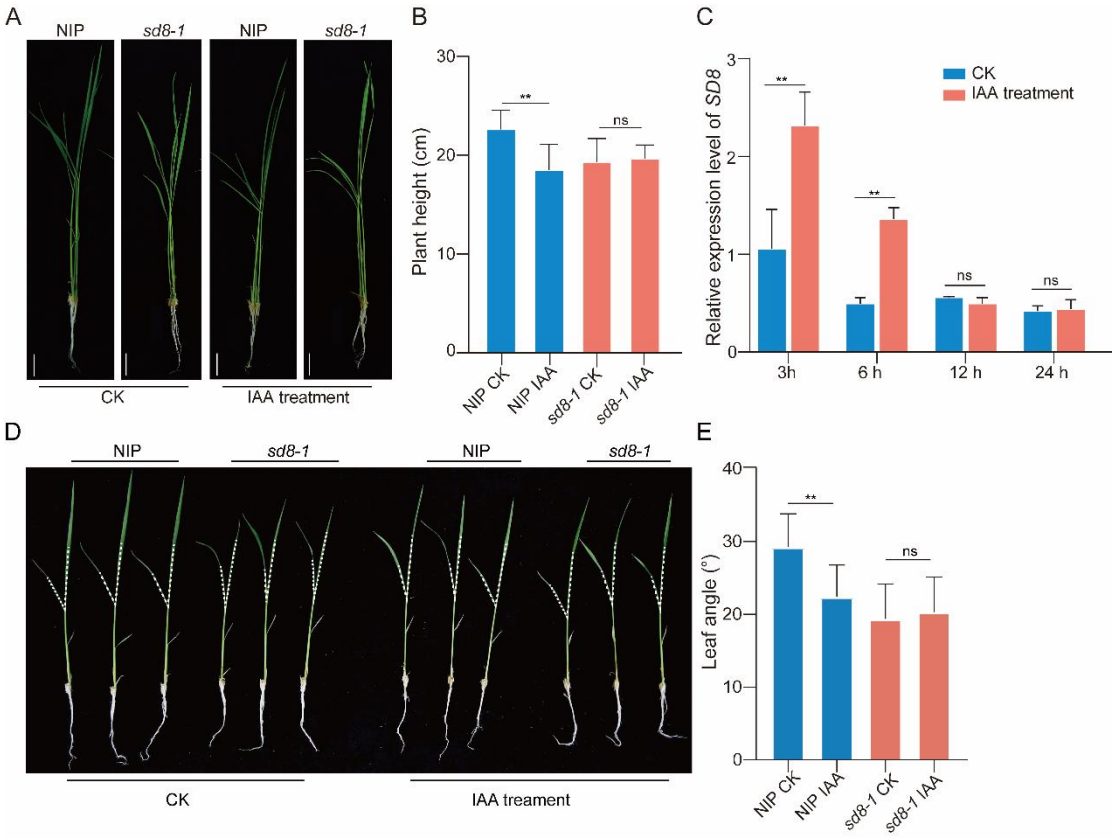


**Supplementary Figure 6. Analysis of auxin response in NIP and *sd8-1*.**

**(A)** Phenotype of NIP and *sd8-1* for 10-day-old seedlings under normal conditions (CK) and 10 μM IAA treatments 3 days. (Scale bars:2 cm).

**(B)** Statistical data of shoot length in NIP and *sd8-1* under 10 μM concentrations of IAA 3days.

**(C)** Expression of *SD8* in 10 μM IAA treatments at the indicated time intervals. 10-day-old seedlings grown in normal culture solution were exposed to 10 μM IAA treatments until shoots were sampled at the indicated time intervals. qRT-PCR experiments were analyzed using three independent biological repeats. The *OsACTIN* gene was used as an internal control.

**(D)** Phenotype of NIP and *sd8-1* for 7-day-old seedlings under normal conditions (CK) and 10 μM IAA treatments 4 days.

**(E)** Statistical data of leaf angle in NIP and *sd8-1* under 10 μM concentrations of IAA 4 days. Data represent mean ± SD (n=35). (**$p < 0.01$; *$p < 0.05$, Student's t-test).

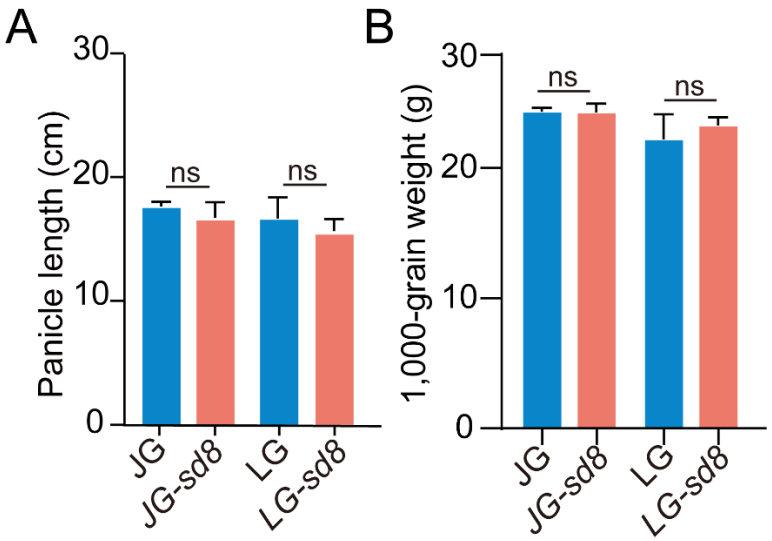


**Supplementary Figure 7. Statistical data of plant height and 1,000-grain weight in wild type and *SD8* KO lines in the indicated backgrounds.**

**(A)** Statistical data of plant height in wild type and *SD8* KO lines in JG and LG.

**(B)** Statistical data of 1,000-grain weight in wild type and *SD8* KO lines in JG and LG. (**$p < 0.01$; *$p < 0.05$, Student's *t*-test).

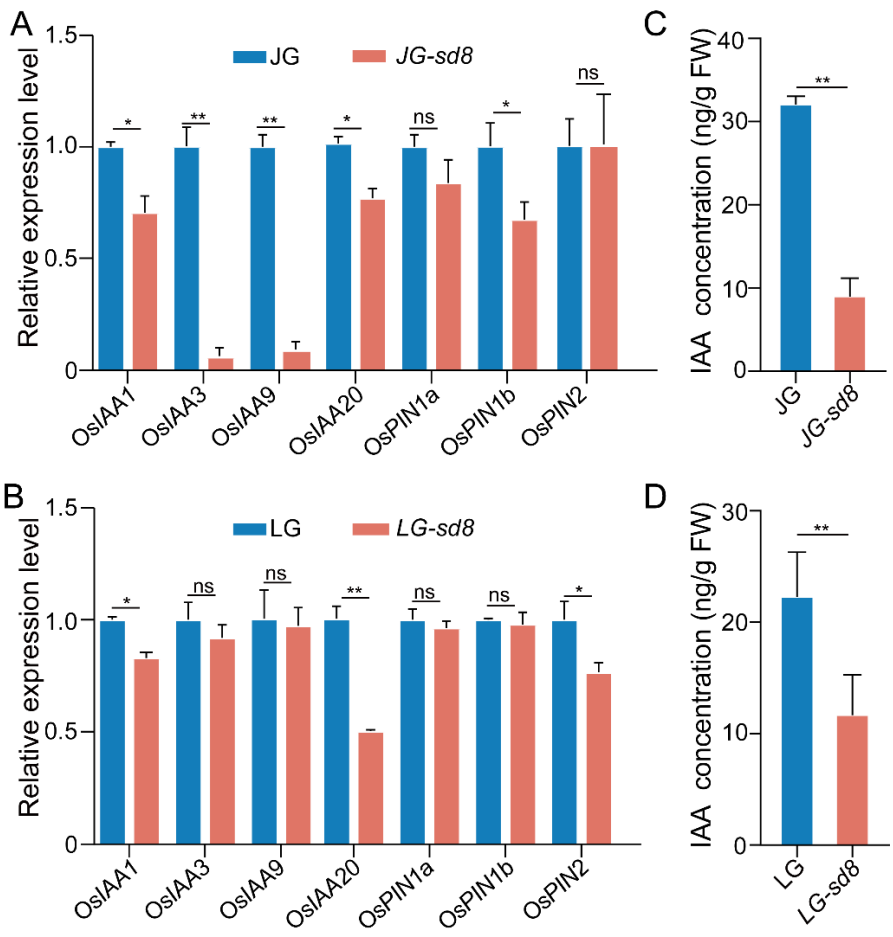


**Supplementary Figure 8. qRT-PCR analysis for auxin-responsive genes and the relative content of free IAA in JG, *JG-sd8*, LG, and *LG-sd8* lines.**

**(A-B)** Relative expression levels of *OsIAA1/3/9/20* and *OsPIN1a/1b/2* in 3-week-old seedlings of JG, *JG-sd8* (A), LG, and *LG-sd8* lines (B) *OsACTIN* gene was used as an internal control. All qRT-PCR experiments were analyzed using three independent biological repeats. (**$p < 0.01$; *$p < 0.05$, Student's *t*-test).

**(C-D)** The relative content of free IAA in 3-week-old seedlings of JG, *JG-sd8*(C), LG, and *LG-sd8* lines (D).

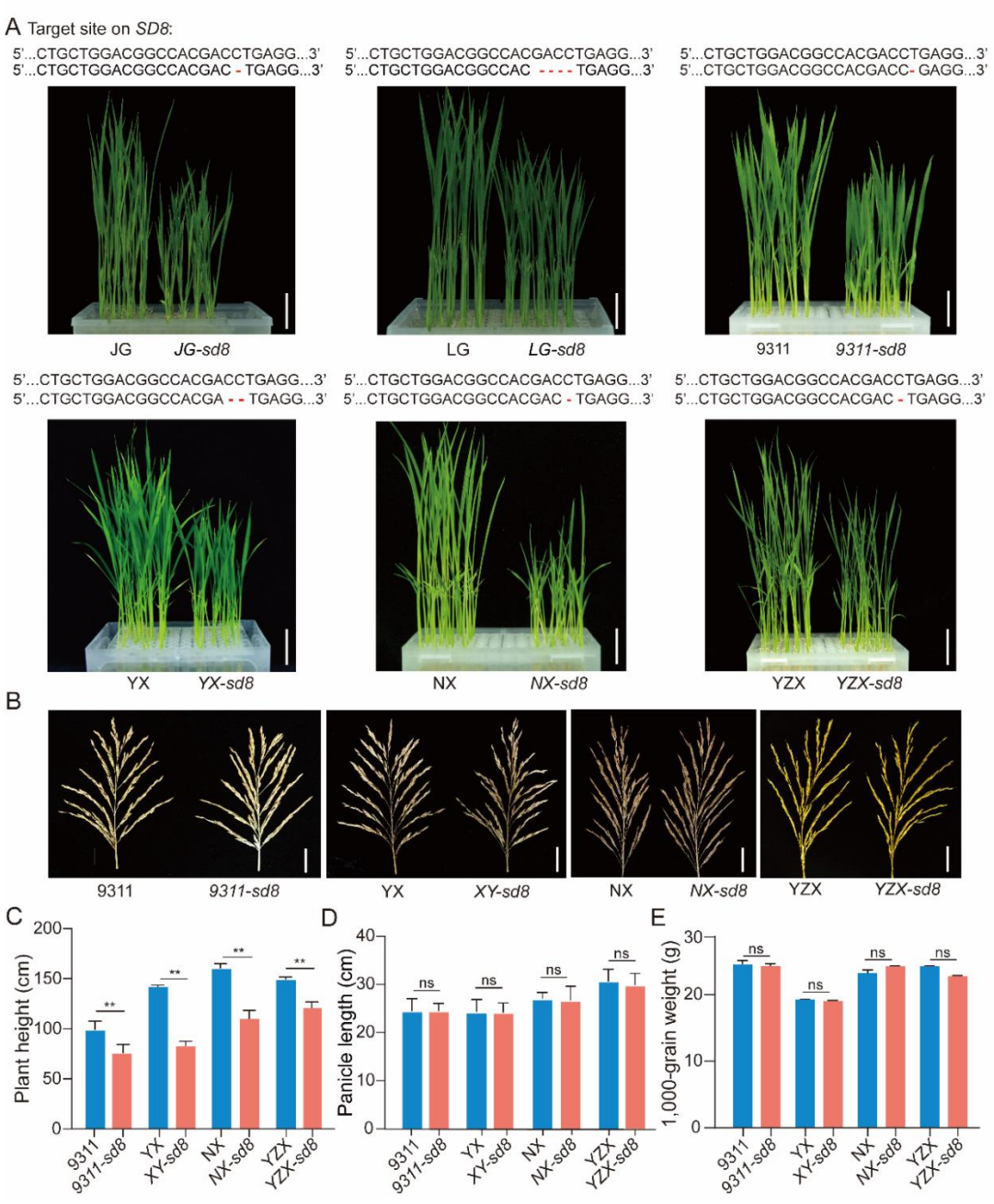


**Supplementary Figure 9. *SD8* KO lines in *japonica* rice variety Jingeng818 (JG), Longgeng 31 (LG) and *indica* rice variety 93-11, YexiangB (YX), Nongxiang32 (NX), and Yuzhenxiang (YZX) backgrounds.**

**(A)** Phenotypes of *SD8* KO lines in the indicated backgrounds. (Scale bars:2 cm).

**(B)** Panicle phenotype of wild type and *SD8* KO lines in NX, 9311, YX, and YZX backgrounds. (Scale bars:5 cm).

**(C)** Statistical data of plant height in wild type and *SD8* KO lines in 9311, YX, YZX, and NX.

**(D)** Statistical data of panicle length in wild type and *SD8* KO lines in the indicated backgrounds.

**(E)** Statistical data of 1,000-grain weight in wild type and *SD8* KO lines in the indicated backgrounds. (**$p < 0.01$; *$p < 0.05$, Student's *t*-test).

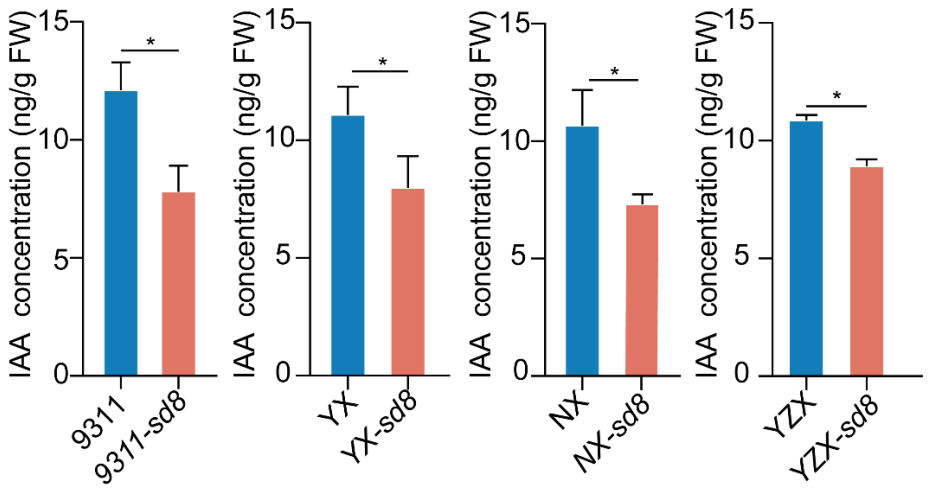


**Supplementary Figure 10. The relative content of free IAA in wild type and *SD8* KO lines in the indicated backgrounds.** GC-MS analysis of endogenous free IAA concentrations in wild type and *SD8* KO lines in the indicated backgrounds. All experiments were analyzed using three independent biological repeats. (**$p < 0.01$; *$p < 0.05$, Student's *t*-test).

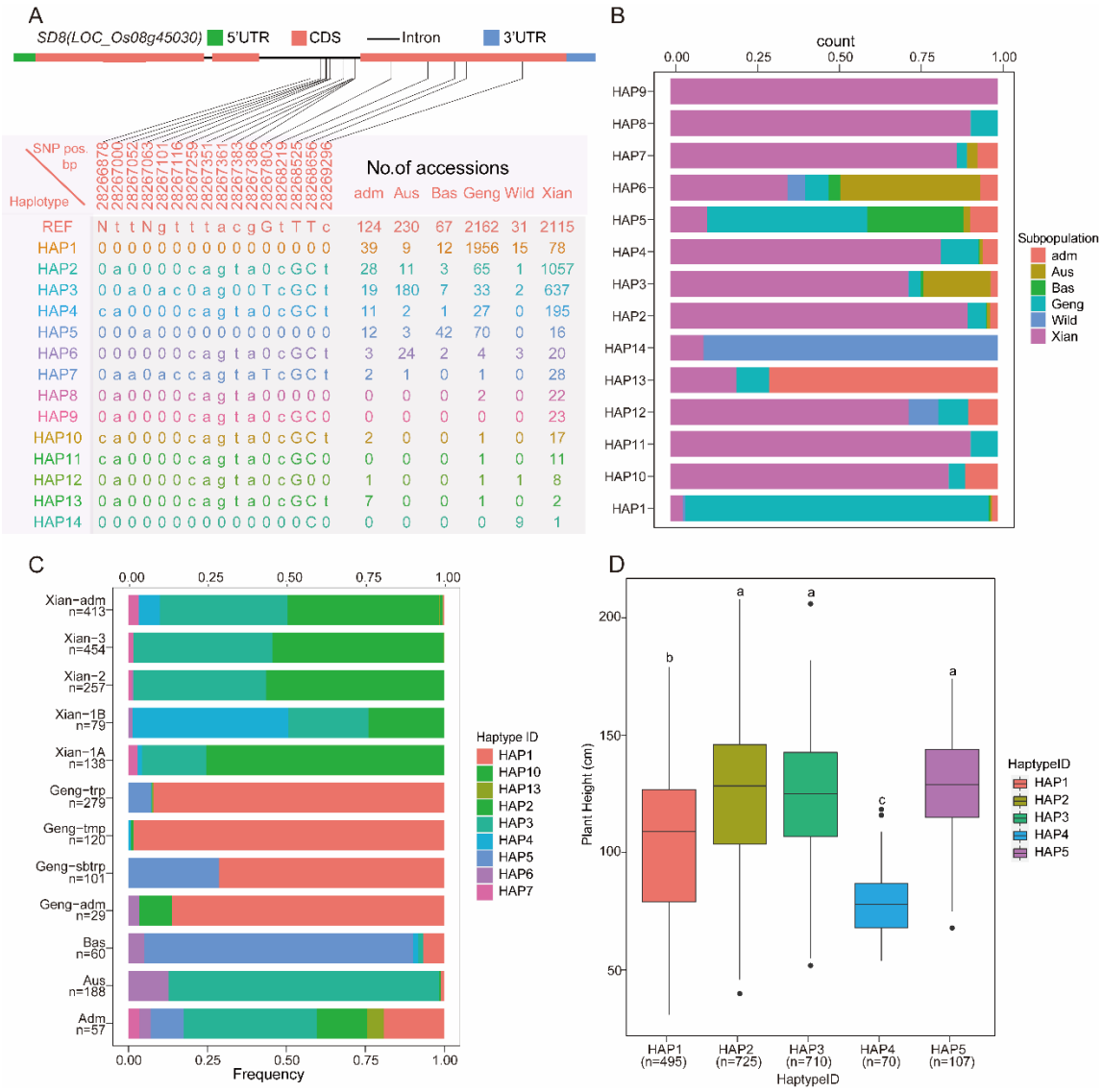


**Supplementary Figure 11. Genetic diversity of *SD8* in the 3K RG dataset.**

**(A)** Haplotypes of *SD8* (*LOC_Os08g45030*) in 1,978 accessions of 3K RG (rare haplotypes of <100 accessions are not shown) using 5 SNPs in the CDS region. Lowercase letters represent synonymous mutations, whereas uppercase letters indicate non-synonymous mutations.

**(B)** Haplotype network of *SD8* in 3K RG.

**(C)** Haplotype frequency of *SD8* in subpopulations of 3K RG.

**(D)** Performance distribution of different haplotypes of *SD8* in 3K RG. Different letters on plant height in 3K RG. Different letters on the boxplots indicate statistically significant differences (n = Hap number; $p$<0.01, Duncan's new multiple range tests).

292 **Table S1.** The primers for qRT-PCR analysis of *SD8*, *OsIAAs*, *OsPINs*.

| Gene name | Forward primer 5'-3' | Reverse primer 5'-3' |
|---|---|---|
| *SD8* | CTGTCCAGCACCTCTTCTGG | GTCCTCCATGTCGAACCAGG |
| *OsIAA1* | GCCGCTCAATGAGGCATT | GCTTCCACTTTCTTTCAATCCAA |
| *OsIAA3* | AACTGAACAACAACAAGAAGAA | GCAATGAGGAGATGAGATGA |
| *OsIAA9* | AAGAAAATGGCCAATGATGATCA | CCCATCACCATCCTCGTAGGT |
| *OsIAA9* | TTGTACGTGAACGGGATTATTTTG | CATGCTTATGAAATTGCTGAAACA |
| *OsPIN1a* | TCATCTGGTCGCTCGTCTGC | CGAACGTCGCCACCTTGTTC |
| *OsPIN1b* | TGCACCCTAGCATTCTCAGCA | CCCTCCTCCCAAATTCTACTTC |
| *OsPIN2* | CAGGGCTAGGAATGGCTATGT | GCAAACACAAACGGGACAA |

293

294

## SI References


**Geng, Y., Zhang, P., Liu, Q.,Wei, Z., Riaz, A., Chachar, S., and Gu, X.** (2020). Rice homolog of Sin3-associated polypeptide 30, OsSFL1, mediates histone deacetylation to regulate flowering time during short days. Plant Biotechnol. J. **18**:325-327.

**Zhang, P., Zhu, C., Geng, Y., Wang, Y., Yang, Y., Liu, Q., Guo, W., Chachar, S., Riaz, A., Yan, S., et al.** (2021). Rice and *Arabidopsis* homologs of yeast CHROMOSOME TRANSMISSION FIDELITY PROTEIN 4 commonly interact with Polycomb complexes but exert divergent regulatory functions. Plant Cell **33**:1417-1429.

**Henrichs, S., Wang, B., Fukao, Y., Zhu, J., Charrier, L., Bailly, A., Oehring, S.C., Linnert, M., Weiwad, M., Endler, A., et al. (2012).** Regulation of ABCB1/PGP1-catalysed auxin transport by linker phosphorylation. EMBO J. **31**:2965-2980.

**Alexandrov, N., Tai, S., Wang, W., Mansueto, L., Palis, K., Fuentes, RR., Ulat, VJ., Chebotarov, D., Zhang, G., Li, Z., et al.** (2015). SNP-Seek database of SNPs derived from 3000 rice genomes. Nucleic Acids Res. **43**:1023-1027.

**Vilella, A., Blanco-Garcia, A.,Hutter, S., Rozas, J.** (2005). Analysis of evolutionary patterns from large-scale DNA sequence polymorphism data. Bioinformatics. **21**:2791–2793.

**Yang, T., Feng, H., Zhang, S., Xiao, H., Xu, G.** (2020). Potassium transporter OsHAK5 alters rice architecture via ATP-dependent transmembrane auxin fluxes. Plant Com. **1**:100052.

**Prusty, R., Grisafi, P., Fink, G.R.** (2004). The plant hormone indoleacetic acid induces invasive growth in Saccharomyces cerevisiae. Proc. Natl. Acad. Sci. U S A. **101**:4153–4157.

**Yang, T., Zhang, S., Hu, Y., Wu, F., Hu, Q., Chen, G., Cai, J., Wu, T., Moran, N., Yu, L., et al.** (2014). The role of a potassium transporter OsHAK5 in potassium acquisition and transport from roots to shoots in rice at low potassium supply

levels. Plant Physiol. **166**:945–957.

**Wang, W., Mauleon, R., Hu, Z., Chebotarov, D., Tai, S., Wu, Z., Li, M., Zheng, T., Fuentes, RR., Zhang, F., et al.** (2018). Genomic variation in 3,010 diverse accessions of Asian cultivated rice. Nature **557**:43-49.

**Bradbury, PJ., Zhang, Z., Kroon, D.E., Casstevens, T.M., Ramdoss, Y., Buckler, E. S.** (2007). TASSEL: software for association mapping of complex traits in diverse samples. Bioinformatics. **23**:2633.

**Duan, P., Xu, J., Zeng, D., Zhang, B., Geng, M., Zhang, G., Huang, K., Huang, L., Xu, R., Ge, S., et al.** (2017). Natural variation in the promoter of GSE5 contributes to grain size diversity in rice. Mol. Plant **10**:685-694.